

# Aspects of dissolved inorganic carbon dynamics in the upwelling system off the Galician coast

Alberto V. Borges\*, Michel Frankignoulle

*Unité d'Océanographie Chimique, Institut de Physique B5, Université de Liège, B4000 Liège, Sart Tilman, Belgium*

Received 30 November 2000; accepted 20 August 2001

## Abstract

In the present paper, we report data on the partial pressure of CO<sub>2</sub> (*p*CO<sub>2</sub>) in surface seawater off the Galician coast, obtained during four cruises carried out in summer (upwelling conditions). Over the continental shelf, two processes that have opposite effects control *p*CO<sub>2</sub> in surface waters: (a) the input from upwelling of deep cold water with high CO<sub>2</sub> content that causes oversaturation of CO<sub>2</sub> and (b) primary production that tends to decrease *p*CO<sub>2</sub>. In offshore waters, the distribution of *p*CO<sub>2</sub> is mainly controlled by temperature change. In two distinct hydrographic coastal regions, the Rías Baixas area (RBA) and the Cape Finisterre area (CFA), the patterns of the distribution of *p*CO<sub>2</sub> are complex but, in the Rías Baixas area, the averaged *p*CO<sub>2</sub> values are systematically lower and temperature values higher. These differences between the two hydrographic regions are mainly related to the combination of outwelling from the Rías and the width of the continental shelf. In the Rías Baixas area, outwelling affects significantly the adjacent inner continental shelf but to a much lesser extent the outer continental shelf. In the Cape Finisterre area, the continental shelf is narrower and the ratio between the surface area of the shelf to the length of the shelf break is lower, inducing during an upwelling event, lower temperature and higher *p*CO<sub>2</sub> values in surface waters than in the Rías Baixas area. © 2002 Elsevier Science B.V. All rights reserved.

*Keywords:* *p*CO<sub>2</sub>; Upwelling; Continental margin exchange; Galician coast

## 1. Introduction

Tsunogai et al. (1999) and Wang et al. (2000) have recently shown that the East China Sea is a sink of atmospheric CO<sub>2</sub> with net annual air–sea fluxes of CO<sub>2</sub> ranging between  $-3.3$  and  $-7.7$  mmol C m<sup>-2</sup> day<sup>-1</sup>. These results led Tsunogai et al. (1999) to formulate the concept of the “continental shelf pump”, i.e. a net influx between 0.5 and 1.0 Gt C year<sup>-1</sup>, if

these air–sea fluxes are extrapolated to the worldwide continental shelf surface area. Frankignoulle and Borges (2001) found similar net annual air–sea fluxes in the Gulf of Biscay, which extrapolated to the surface area of the Northern European continental shelf give an additional net influx of atmospheric CO<sub>2</sub> of about 45% to the influx estimated by Takahashi et al. (1995) and Sarmiento et al. (1995) for the open North Atlantic Ocean. These results are based on high temporal and spatial resolution data sets of direct measurements of the gradient of CO<sub>2</sub> across the air–sea interface and show that continental shelves are a significant component of the global carbon cycle. This assertion is corroborated by other studies based on various indirect

\* Corresponding author. Tel.: +32-4-3663367; fax: +32-4-3662355.

*E-mail address:* Alberto.Borges@ulg.ac.be (A.V. Borges).

approaches such as the budget of carbon fluxes across the continental shelf margin (Walsh, 1988, 1991; Wollast, 1998), the net ecosystem metabolism of continental shelves (Gattuso et al., 1998) and a carbon biogeochemical model calibrated with  $p\text{CO}_2$  field data in the Baltic Sea (Thomas and Schneider, 1999).

Upwelling systems are characterised by high primary production rates ranging from 60 to 2000  $\text{g C}^{-2}$   $\text{year}^{-1}$  off the Moroccan and Chilean coasts, respectively, making these areas sites of significant carbon fluxes across the continental shelf margin (e.g. Walsh, 1988; Alongi, 1988; Álvarez-Salgado et al., 2002). Upwelling brings to the surface deep water with a high  $\text{CO}_2$  content that induces oversaturation of  $\text{CO}_2$  with respect to the atmosphere. For instance, in the Peruvian and Chilean coastal upwelling systems that are known to be among the most productive oceanic areas worldwide, huge oversaturation of  $\text{CO}_2$  with respect to the atmosphere has been reported with  $p\text{CO}_2$  values up to 1200  $\mu\text{atm}$ , although very low values down to 140  $\mu\text{atm}$  have also been observed in relation to dissolved inorganic carbon fixation by phytoplankton (Kelley and Hood, 1971; Simpson and Zirino, 1980; Copin-Montégut and Raimbault, 1994; Torres et al., 1999). Other coastal upwelling systems also show a wide range of  $p\text{CO}_2$  values such as 130–690  $\mu\text{atm}$  off the California coast (Simpson, 1984; van Green et al., 2000), 300–450  $\mu\text{atm}$  off the Mauritanian coast (Copin-Montégut and Avril, 1995; Lefèvre et al., 1998; Bakker et al., 1999) and 365–750  $\mu\text{atm}$  off the Omani coast (Körtzinger et al., 1997; Goyet et al., 1998). This variability is due to the opposing effects of upwelling and primary production on surface water  $p\text{CO}_2$ , which also induce strong spatial heterogeneity as illustrated by high-resolution surface mapping off the Portuguese, the Californian and the Galician coasts (Pérez et al., 1999; van Green et al., 2000; Borges and Frankignoulle, in press). In general, the available data sets do not fully cover the annual cycle so that it is unclear if upwelling systems behave, at an annual basis, as sinks or sources of atmospheric  $\text{CO}_2$ .

In a recent paper, Borges and Frankignoulle (in press) report the distribution of surface water  $p\text{CO}_2$  off the Galician coast (Northwestern Spain) obtained during six cruises. Surface water  $p\text{CO}_2$  values over the continental shelf range between 265 and 415  $\mu\text{atm}$  during summer (upwelling season) and between 316 and 345  $\mu\text{atm}$  during winter (downwelling season).

The computed air–sea fluxes of  $\text{CO}_2$  over the continental shelf yield a net influx in the range of  $-2.3$  to  $-4.7$   $\text{mmol C m}^{-2} \text{day}^{-1}$  during the upwelling season and  $-3.5$  to  $-7.0$   $\text{mmol C m}^{-2} \text{day}^{-1}$  at an annual basis for the Liss and Merlivat (1986) and the Tans et al. (1990) formulations of the  $\text{CO}_2$  exchange coefficient, respectively. One of the aspects of the distribution of surface water  $p\text{CO}_2$  over the Galician continental shelf highlighted by Borges and Frankignoulle (in press) is the contrast between the northern area of the sampling region situated off Cape Finisterre and the southern area situated off the Rías Baixas (i.e. coastal indentations). For any given summer cruise, the (spatially) averaged  $p\text{CO}_2$  values are lower and temperature higher off the Rías Baixas than off Cape Finisterre, where oversaturation of  $\text{CO}_2$  related to upwelling was observed during all four summer cruises. The fact that the contrast between these two hydrographic regions was observed during all cruises strongly suggests that it is not coincidental but a systematic feature.

The most straightforward hypothesis to explain the contrast between the two hydrographic regions is the presence of the Rías Baixas themselves. During the upwelling season, when the input of fresh water is relatively low ( $<10 \text{ m}^3 \text{ s}^{-1}$ , Nogueira et al., 1997), the Rías Baixas function as an extension of the continental shelf and not as rivers or estuaries. This means that upwelling occurs within the Rías as first described by Fraga (1981) and clearly evidenced by numerous studies (e.g. Álvarez-Salgado et al., 1993, 1999; Doval et al., 1997; Nogueira et al., 1997, 1998). The water circulation in the Rías is two layered, the bottom layer corresponding to upwelled Eastern North Atlantic Water (ENAW) that enters the Ría during an upwelling event and pushes the surface layer water out of the Ría. This phenomenon is described in literature as “outwelling” from the Rías. The outwelled surface water is modified ENAW that entered the Ría during the upwelling event of the previous upwelling cycle (period typically of 14 days, Álvarez-Salgado et al., 1993). Thus, the physico-chemical and biological characteristics of this water mass are related to the relaxation stage that preceded the on-going upwelling event. The outwelled water is warm and has undergone high primary production (e.g. Tilstone et al., 1999) related to the input of nutrients from upwelled ENAW, to sediment remineralization and to a lesser extent by

the input of fresh water (e.g. Álvarez-Salgado et al., 1993).

The purpose of the present work is to discuss some aspects of dissolved inorganic carbon dynamics based on data collected during four cruises carried out off the Galician coast during the upwelling season as a contribution to the Ocean Margin EXchange (OMEX II) project. In Section 3.1, the main processes that control  $p\text{CO}_2$  over the continental shelf and in the off-shore waters of the Galician coastal upwelling system are described and discussed. In Section 3.2, the potential influence of the Rías to explain the difference between the two hydrographic regions over the continental shelf is explored by the analysis of data obtained within and around the Ría of Vigo. In Section 3.3, with simple simulations, we explore the hypothesis of the effect of the width of the continental shelf to explain the difference between the two continental shelf hydrographic regions. Finally, in Section 3.4, we examine the possibility that the difference between the two hydrographic regions over the continental shelf could be related to the synopticity of sampling and bias in data integration.

## 2. Materials and methods

Data presented in this paper were obtained on board the *R.V. Belgica* and the *R.R.S. Charles Darwin* during four cruises (Belgica 97/14–18/06 to 07/07/97, Belgica 98/15–14/06 to 14/07/98, CD114–29/07 to 24/08/98 and Belgica 99/19–30/08 to 21/09/99). Underway parameters (seawater  $p\text{CO}_2$ , dissolved oxygen, salinity, in situ temperature and fluorescence) were sampled with a frequency of 1 min from the nontoxic seawater supply of the ship (pump inlet at  $-2.5$  m). A non-dispersive infrared gas analyser (Li-Cor®, LI-6262) was used to measure  $p\text{CO}_2$  in wet air equilibrated with seawater. Before 1998,  $p\text{CO}_2$  was measured in equilibrated air dried with Drierite® and the data were converted into wet air using the algorithms proposed by DOE (1994). The Li-Cor® was calibrated daily using three gas standards of 0.0  $\mu\text{atm}$  (pure nitrogen, Air Liquide Belgium), 351.0  $\mu\text{atm}$  (Air Liquide Belgium) and 360.5  $\mu\text{atm}$  (National Oceanic and Atmospheric Administration). The  $p\text{CO}_2$  values are corrected for the temperature difference between in situ seawater and water in the equilibrator, using the algorithm

proposed by Copin-Montégut (1988) (the offset in temperature was typically  $\sim 0.5$  °C). More details on the equilibration technique, equilibrator design and quality control can be found in Frankignoulle et al. (2001). The accuracy of the  $p\text{CO}_2$  measurement by equilibration is estimated to  $\pm 2$   $\mu\text{atm}$  (including cumulated uncertainties on temperature correction and instrument calibration). A second Li-Cor® was used to measure atmospheric  $p\text{CO}_2$  sampled at the bow of the ship at approximately 10 m height. Total Alkalinity (TAlk) was determined using the classical Gran electrotitration method, on 100 ml GF/F filtered samples. The precision of TAlk measurements obtained on board is  $\pm 4$   $\mu\text{mol kg}^{-1}$ . The measurement of pH was obtained using a Ross combination electrode (ORION®), calibrated on the Total Hydrogen Ion Concentration Scale ( $\text{mol kg SW}^{-1}$ ), using the TRIS and AMP buffers proposed by Dickson (1993). The precision of the pH measurement is estimated to be  $\pm 0.004$  pH units. Total dissolved inorganic carbon (DIC) was calculated from the pH and TAlk measurements with the dissociation constants of carbonic acid from Roy et al. (1993), the borate molality obtained from the Culkin (1965) ratio to salinity, the dissociation constant of boric acid from Dickson (1990) and the carbon dioxide solubility coefficient of Weiss (1974), with an estimated accuracy of  $\pm 5$   $\mu\text{mol kg}^{-1}$ . Underway dissolved oxygen was measured using a galvanic electrode (Kent®) calibrated, every 12 h, from discrete samples measured by the Winkler method using a potentiometric endpoint determination, with an estimated accuracy of  $\pm 2$   $\mu\text{mol kg}^{-1}$  ( $\pm 0.5\%$  of level of saturation). The oxygen saturation level (% $\text{O}_2$ ) is computed from the observed concentration of dissolved  $\text{O}_2$  and the concentration of  $\text{O}_2$  at saturation calculated using the algorithm proposed by Benson and Krause (1984). The concentration of chlorophyll *a* was determined from GF/F filtered samples, by the fluorimetric method (Arar and Collins, 1997), with a precision of  $\pm 4\%$ . Underway fluorescence was determined with a Turner Designs® 10AU fluorimeter. Salinity and in situ temperature were measured using a SeaBird® 21 (*Belgica*) and a Falmouth Scientific Instruments® (*Charles Darwin*) thermosalinograph, with an estimated accuracy of  $\pm 0.05$  and  $\pm 0.01$  °C, respectively. Vertical profile data were obtained from a 12 bottle rosette coupled to a CTD (SeaBird® 19).

### 3. Results and discussion

#### 3.1. Spatial and temporal variability of $p\text{CO}_2$ in the off-shore and the continental shelf waters off the Galician coast

##### 3.1.1. General setting and characterization of the different hydrographic regions

Table 1 summarizes the atmospheric and seawater  $p\text{CO}_2$  and temperature data obtained during four cruises carried out off the Galician coast during summer. For each cruise, the data were separated into four hydrographic regions, the Cape Finisterre area (CFA), the Rías Baixas area (RBA), the Coastal Transition Zone (i.e. upwelling filaments, CTZ) and the remaining off-shore area (OSA) shown in Fig. 1. Upwelling occurred during all four cruises but with variable intensity. As shown by average surface water temperature, the June 1997 cruise corresponded to the transition of strong upwelling relaxation to moderate active upwelling conditions, the first leg of the September 1999 cruise (from the 4th to the 11th) corresponded to strong upwelling relaxation conditions, while the remaining cruises corresponded to strong

active upwelling conditions. In spite of a wide range of  $p\text{CO}_2$  and temperature values, the (spatially) averaged values in the RBA are systematically lower for  $p\text{CO}_2$  and higher for temperature than in the CFA. The averaged values in the CTZ are systematically lower for  $p\text{CO}_2$  and temperature than in the OSA.

Atmospheric  $p\text{CO}_2$  data for any given cruise show a wide range of values. This can be explained by the presence of air masses of offshore and of continental origin, as discussed in detail by Borges and Frankignoulle (2002b). Interestingly, a decrease of both the average value and the range of variability was observed from the first to the second leg of the September 1999 cruise. This could be explained by the southward winds associated to the active upwelling event that occurred during the second leg of the cruise that brought into the study region an air mass with offshore and oceanic characteristics (most probably from the Gulf of Biscay).

##### 3.1.2. Property–property plots

Fig. 2 shows surface water parameters from two selected summer cruises plotted versus temperature, a convenient way to analyse data in upwelling areas.

Table 1

Summary of averaged values of water temperature ( $^{\circ}\text{C}$ ), surface seawater  $p\text{CO}_2$  ( $\mu\text{atm}$ ), the air–sea gradient of  $\text{CO}_2$  ( $\Delta p\text{CO}_2$ ) and atmospheric  $p\text{CO}_2$ , obtained off the Galician coast during four summer cruises

Cruise	Region	Water temperature	Seawater $p\text{CO}_2$	$\Delta p\text{CO}_2$	Atmospheric $p\text{CO}_2$
21 June–2 July 1997 (upwelling relaxation)	CFA	16.6 (17.7, 14.2)	337 (386, 289)	–27	362 (363, 362)
	RBA	17.7 (19.0, 15.2)	324 (343, 266)	–36	
	OSA	18.2 (19.2, 17.5)	338 (346, 328)	–23	
27 June–7 July 1998 (active upwelling)	CFA	14.1 (16.0, 13.4)	358 (397, 263)	–1	359 (373, 354)
	RBA	15.3 (17.2, 13.5)	315 (384, 274)	–46	
	CTZ	17.2 (17.5, 14.1)	331 (367, 308)	–27	
	OSA	17.8 (18.8, 17.5)	342 (359, 329)	–18	
11–21 August 1998 (active upwelling)	CFA	14.1 (15.8, 13.1)	352 (383, 322)	+2	353 (364, 348)
	RBA	14.8 (16.9, 13.0)	341 (390, 310)	–14	
	CTZ	15.8 (17.5, 14.1)	326 (349, 302)	–28	
	OSA	18.2 (19.7, 17.5)	339 (351, 329)	–14	
4–11 September 1999 (upwelling relaxation)	CFA	16.7 (17.7, 15.6)	351 (384, 315)	–14	365 (392, 343)
	RBA	18.4 (19.8, 16.5)	349 (364, 306)	–18	
	CTZ	16.9 (17.5, 15.3)	344 (381, 321)	–15	
	OSA	19.6 (21.2, 17.5)	361 (374, 329)	+1	
14–18 September 1999 (active upwelling)	CFA	15.9 (17.0, 14.5)	356 (415, 267)	–1	357 (369, 355)
	RBA	16.8 (18.4, 15.4)	339 (394, 294)	–19	
	CTZ	17.3 (17.5, 17.1)	341 (346, 334)	–16	
	OSA	18.5 (19.8, 17.5)	351 (363, 337)	–6	

Atmospheric  $p\text{CO}_2$  data for the June 1997 cruise are from Barrow Point (Keeling and Whorf, 1999). Numbers in brackets correspond to maximum and minimum of observed values. The different hydrographic regions are represented in Fig. 1.

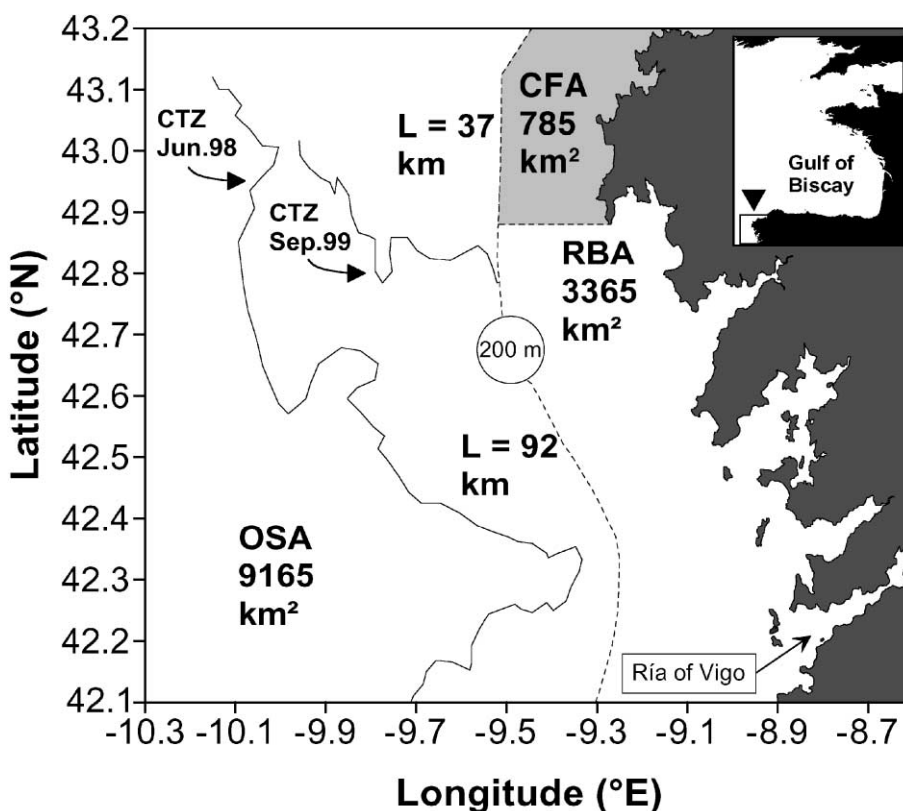
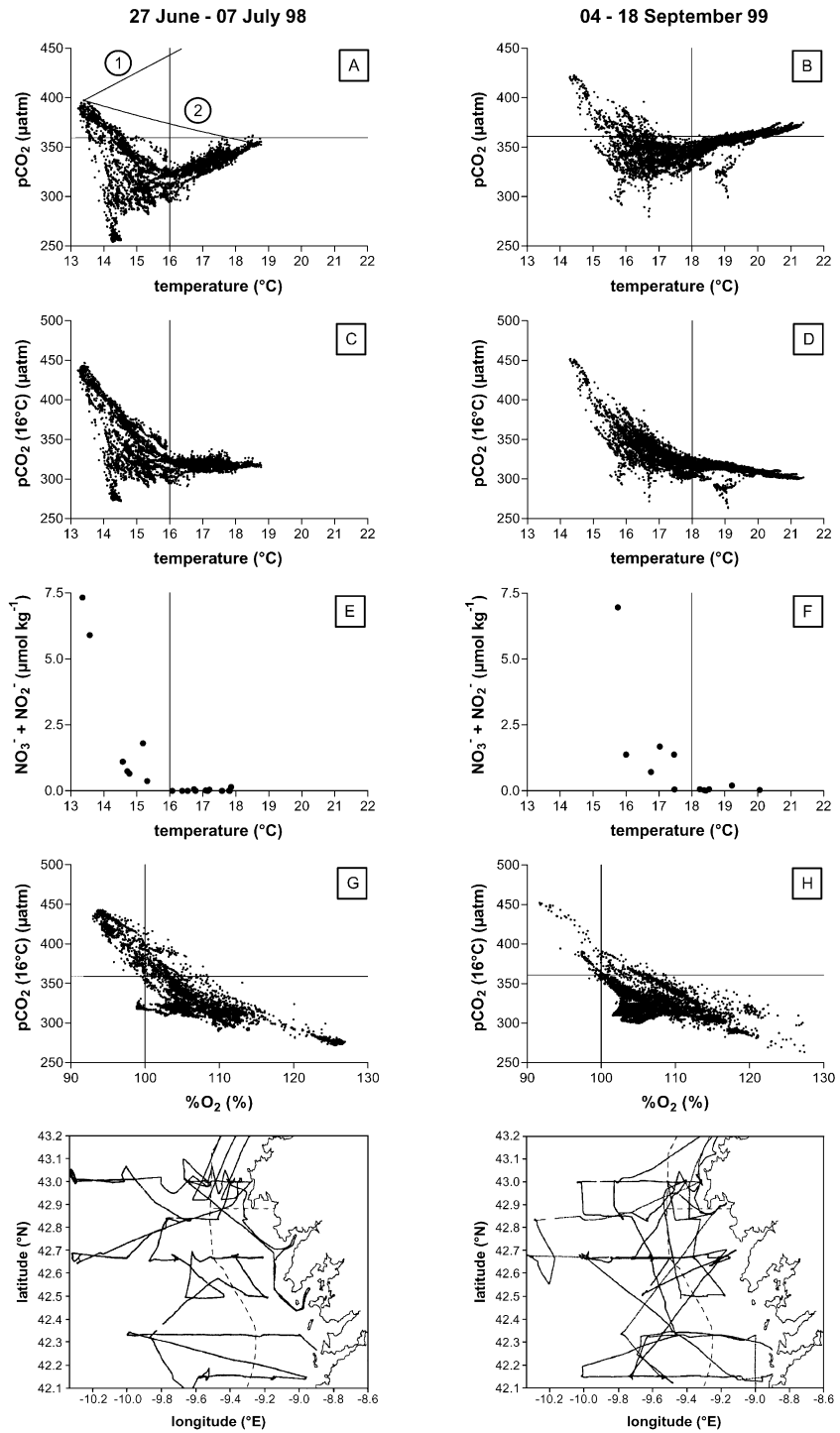


Fig. 1. Location of the study site with the different hydrographic areas and their surface areas: CFA=Cape Finisterre area; RBA=Rías Baixas area; OSA=Offshore area; CTZ=Coastal Transition Zone. The CTZ corresponds to upwelling filaments and is defined as off-shore waters with a surface water temperature lower than 17.5 °C based on Borges and Frankignoulle (2002b).  $L$  is the length of the shelf break for the CFA and the RBA.

Surface water  $p\text{CO}_2$  versus temperature shows a relatively complex pattern; however, some trends are consistent for both cruises, as, for instance, the highest  $p\text{CO}_2$  values associated to the lowest temperature as expected in a system where upwelling brings to the surface cold, deep and  $\text{CO}_2$ -rich water (Fig. 2A,B). The lowest  $p\text{CO}_2$  values are associated to intermediate temperatures. In the high temperature range, surface seawater is close to atmospheric equilibrium.

For the June 1998 cruise, the theoretical evolution of a water parcel characterized by the highest  $p\text{CO}_2$  value (397  $\mu\text{atm}$  at 13.4 °C) was computed in the one hand when allowed to warm and in the other hand when allowed to mix with a water parcel with the highest temperature ( $p\text{CO}_2=352$   $\mu\text{atm}$  at 18.8 °C), assuming that salinity and Total Alkalinity remain constant at 35.7 and 2.340  $\text{mmol kg}^{-1}$ , respectively.

It is clear that the observed  $p\text{CO}_2$  data points do not follow either of these theoretical curves (lines 1 and 2 in Fig. 2A), which is due to the effect of net phytoplanktonic fixation of dissolved inorganic carbon, as the temperature increases, i.e. as the water mass ages. This is corroborated by the good relationship between  $p\text{CO}_2$  normalized to an average temperature of 16 °C [ $p\text{CO}_2(16\text{ °C})$ ] and % $\text{O}_2$  (Fig. 2G,H). It should be noted that at the time scale of 14 days (the periodicity of the cycle of active upwelling and upwelling relaxation), the effect of air–sea exchange of  $\text{CO}_2$  can be neglected in relation to other processes such as biological activity. Indeed, if the water parcel characterized by the highest  $p\text{CO}_2$  value (397  $\mu\text{atm}$ ) observed during the June 1998 cruise was allowed to exchange  $\text{CO}_2$  with the atmosphere during 14 days (in absence of other processes), then a decrease of  $p\text{CO}_2$  of only



11  $\mu\text{atm}$  would be observed (for a constant wind speed of  $10 \text{ m s}^{-1}$  (average value during the cruise), using the Wanninkhof (1992) exchange coefficient formulation in a 1-min iterative computation method (for details refer to Borges and Frankignoulle, 2002b) and assuming a mixed layer 20-m deep, temperature =  $13.4 \text{ }^\circ\text{C}$ , salinity = 35.7,  $\text{TALK} = 2.340 \text{ mmol kg}^{-1}$ ). Thus, the potential effect of air–sea  $\text{CO}_2$  exchange is one order of magnitude lower than the variability of  $\sim 100 \mu\text{atm}$  due to other processes.

Depletion of  $\text{NO}_3^-$  is observed at temperatures  $\geq 16$  and  $\geq 18 \text{ }^\circ\text{C}$  for the June 1998 and the September 1999 cruises, respectively (Fig. 2E,F). In a nitrate-depleted mixed layer, new primary production is replaced by regenerated primary production that, in theory, should not correspond to a significant net dissolved inorganic carbon fixation. For both cruises, a  $p\text{CO}_2$  increase is observed with rising temperatures in the nitrate-depleted waters (Fig. 2A,B). However, in the high temperature range, the  $p\text{CO}_2$  ( $16 \text{ }^\circ\text{C}$ ) values remain relatively constant (Fig. 2C,D). This illustrates that the observed increase of  $p\text{CO}_2$  with temperature (Fig. 2A,B), in the nitrate-depleted waters, can be explained by the effect of temperature on the equilibrium constants of dissolved inorganic carbon and, in particular, the solubility coefficient of  $\text{CO}_2$  ( $p\text{CO}_2$  rise of  $\sim 4\%$  with temperature increase of  $1 \text{ }^\circ\text{C}$ ).

### 3.2. Spatial and temporal variability of $p\text{CO}_2$ in the Ría of Vigo and adjacent continental shelf

#### 3.2.1. Vertical variability in front of the Ría of Vigo

Fig. 3 shows vertical profile data obtained by repeated sampling of a station in front of the Ría of Vigo. The temperature profiles show that the various sampling periods correspond to different hydrological conditions: upwelling relaxation (i.e. stratification) on the 22nd of June 1997 and on the 9th of September 1999 and active upwelling on the 28th of June 1998 (Fig. 3A). The salinity profiles show that surface waters are less saline on both the 22nd of June 1997

and the 9th of September 1999, however, on the 28th of June, salinity is fairly constant throughout the water column (Fig. 3B). The  $\% \text{O}_2$  values are higher in surface waters as would be expected from subsurface phytoplanktonic activity as also suggested by the chlorophyll *a* profiles and corroborated by the  $\text{DIC}_{35}$  profiles (Fig. 3C–E). The chlorophyll *a* profiles also suggest higher phytoplanktonic activity associated with active upwelling conditions. Either during active upwelling conditions (28th of June 1997) or upwelling relaxation (22nd of June 1997), very low nitrate concentrations are observed in surface waters ( $\leq 0.7 \mu\text{mol kg}^{-1}$ ). (No nitrate data are available for the 9th of September 1999 but for all three profiles, very low phosphate concentrations were measured in surface waters, with values  $\leq 0.14 \mu\text{mol kg}^{-1}$ , Dr. Lei Chou, personal communication). The  $\% \text{O}_2$  and  $\text{DIC}_{35}$  values below 40 m from the 22nd of June 1997 and the 28th of June 1998 are very close. However, the  $\% \text{O}_2$  and  $\text{DIC}_{35}$  values below 40 m from the 9th of September suggest enhanced degradation processes in the deeper water column. Surface water  $p\text{CO}_2$  values (underway measurements) on the 22nd of June 1997, the 28th of June 1998 and the 9th of September 1999 all show undersaturation: 336, 298 and 327  $\mu\text{atm}$ , respectively. The  $p\text{CO}_2$  ( $16 \text{ }^\circ\text{C}$ ) values are 308, 315 and 293  $\mu\text{atm}$ , respectively, in accordance with surface  $\text{DIC}_{35}$  values: a slightly lower value on the 9th of September and similar values on the two other occasions. Nevertheless, significant undersaturation of  $\text{CO}_2$  is observed during active upwelling, which is due to enhanced primary production as shown above by the chlorophyll *a* and  $\text{DIC}_{35}$  profiles.

The salinity profiles in Fig. 3 suggest an input of fresh water, particularly in September 1999. The TS diagrams in Fig. 4A show that the samples below 50 m fall on the regression line of ENAW that upwells off the Rías Baixas (Fraga et al., 1982). However, the data points above 50 m do not fall on a vertical line as would be expected if surface water were warm ENAW. This is true for all three stations, but more

Fig. 2.  $p\text{CO}_2$  ( $\mu\text{atm}$ ),  $p\text{CO}_2$  normalized to  $16 \text{ }^\circ\text{C}$  ( $\mu\text{atm}$ ) and nitrate versus temperature ( $^\circ\text{C}$ ), and  $p\text{CO}_2$  normalized to  $16 \text{ }^\circ\text{C}$  versus oxygen saturation level (%), for two summer cruises off the Galician coast. The horizontal dotted line corresponds to the  $\text{CO}_2$  atmospheric equilibrium. Solid lines show the theoretical evolutions of a water parcel with the highest  $p\text{CO}_2$  value ( $397 \mu\text{atm}$  at  $13.4 \text{ }^\circ\text{C}$ ) when allowed to warm (line 1) and when allowed to mix with a water parcel with the highest temperature ( $p\text{CO}_2 = 352 \mu\text{atm}$  at  $18.8 \text{ }^\circ\text{C}$ ) (line 2). Nutrient data are courtesy of Drs. X.A. Álvarez-Salgado (IIM) and L. Chou (ULB).

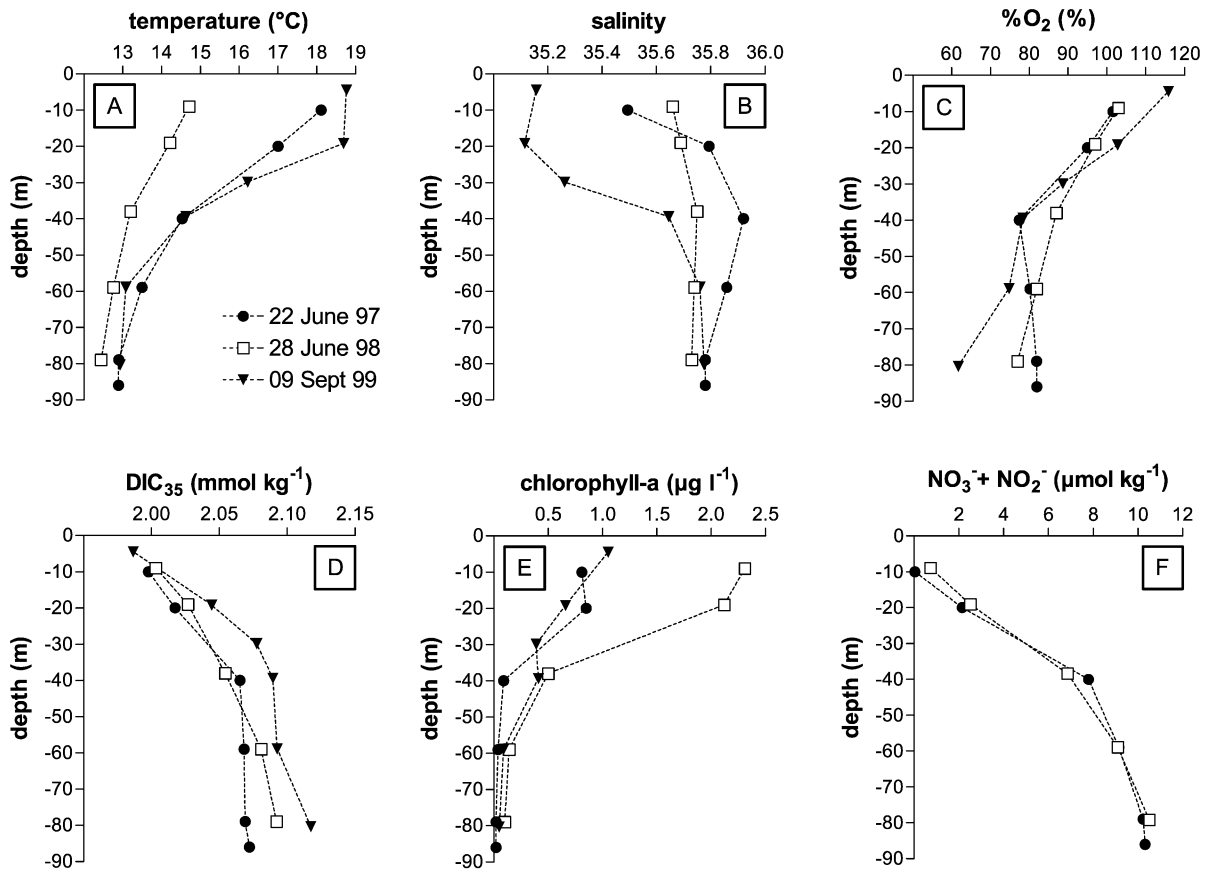


Fig. 3. Vertical profiles of temperature (°C), salinity, oxygen saturation level (%), DIC<sub>35</sub> (mmol kg<sup>-1</sup>), chlorophyll *a* concentration (µg l<sup>-1</sup>) and NO<sub>3</sub><sup>-</sup> + NO<sub>2</sub><sup>-</sup> concentration (µmol kg<sup>-1</sup>), on three occasions at a station (-8.96°E, 42.15°N) located ~5 km away from the mouth of the Ría of Vigo. Chlorophyll *a* data are courtesy of Dr. L. Chou (ULB). Nutrient data are courtesy of Drs. X.A. Álvarez-Salgado (IIM) and M. Elskens (VUB).

pronounced for the two stations sampled during upwelling relaxation. Thus, the water in the surface layer has mixed with a less saline water mass outwelled from the Ría of Vigo. The TS diagrams above the shelf break at the same latitude as the station in front of the Ría of Vigo show that the data points in the surface layer are closer to the expected vertical line (Fig. 4B). This means that the surface water at the shelf break mixed to a lesser extent with water outwelled from the Ría of Vigo. The profile from the June 1997 cruise that corresponded to an intense upwelling relaxation event shows the most pronounced effect from mixing with outwelled water at the shelf break (Fig. 4B).

### 3.2.2. Longitudinal and seasonal variability in the Ría of Vigo and the adjacent continental shelf

To further investigate the role of the Rías Baixas in the study area, Fig. 5 shows all the underway data we collected within and around the Ría of Vigo. These transects cover the continental shelf adjacent to the Ría of Vigo from the shelf break at about -9.3°E to the mouth of the Ría at -8.9°E and the Ría itself up to -8.7°E. The distribution of water temperature shows that sampling was carried out under various hydrographic conditions (Fig. 5B). Temperature is high along the transects carried out on the 20th of June 1997 and the 9th of September 1999 that correspond to upwelling relaxation conditions (see Table 1). The



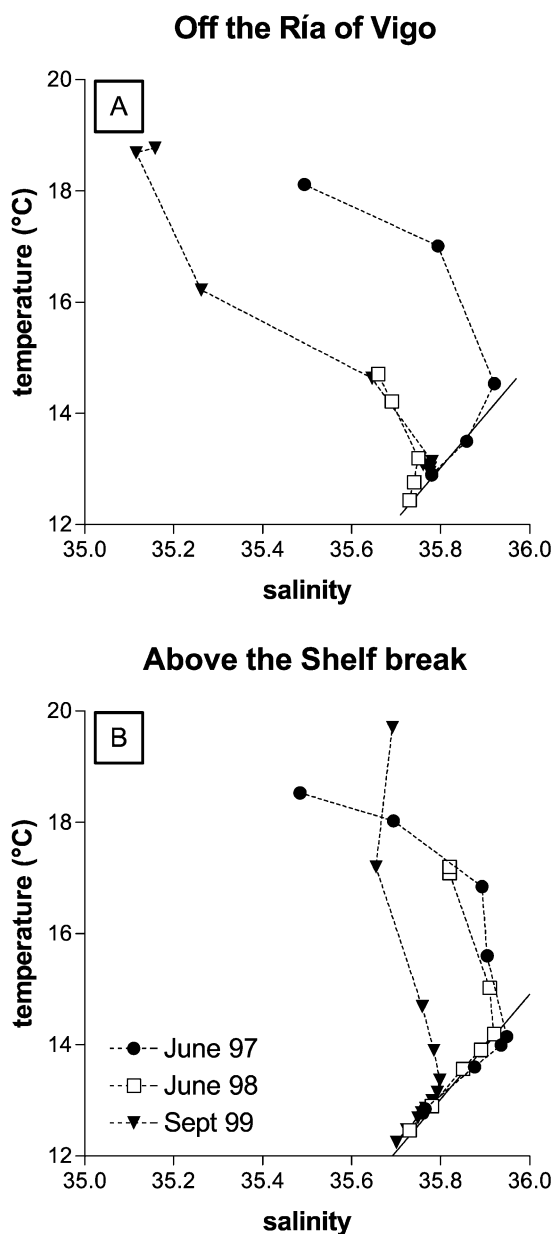


Fig. 4. TS diagrams at a station ( $-8.96^{\circ}\text{E}$ ,  $42.15^{\circ}\text{N}$ ) located  $\sim 5$  km away from the mouth of the Ría of Vigo and at a station at the shelf break ( $-9.30^{\circ}\text{E}$ ,  $42.15^{\circ}\text{N}$ ). Solid line is the regression line of Eastern North Atlantic Water (ENAW,  $S=35.586+0.106(T-11)$ ) according to Fraga et al. (1982).

other transects correspond to active upwelling conditions of variable intensity. The transect carried out on the 20th of August 1998 corresponds to very intense

upwelling conditions with temperatures over the shelf as low as  $15^{\circ}\text{C}$ . However, the relative variation of temperature is as indicative of upwelling intensity as the absolute temperature values. For instance, between the 11th and the 20th of August 1998, water temperature at  $9.1^{\circ}\text{E}$  changed of about  $1.5^{\circ}\text{C}$  ( $\sim 0.2^{\circ}\text{C}$  per day) while between the 9th and the 16th of September 1999 the temperature change was  $2.5^{\circ}\text{C}$ , thus twice more rapid ( $\sim 0.4^{\circ}\text{C}$  per day). Therefore, the transect of the 16th of September 1999 can also be associated to strong active upwelling conditions. For the two upwelling relaxation transects (20th of June 1997 and the 9th of September 1999), the distribution of temperature is fairly homogeneous along the transect, while for the transects carried out during active upwelling conditions, the temperature within the Ría of Vigo is generally higher than over the adjacent continental shelf. This can be related to the fact that the Ría of Vigo is shallower ( $\leq 50$  m) and more protected from wind speed (i.e. less turbulent) than the adjacent continental shelf, so that surface water will warm more rapidly. This means that the surface water mass on the continental shelf is only partly outwelled from the Ría; otherwise, it would be at the same temperature as the one of the Ría. We can conclude that during an upwelling event, the outwelled water from the Ría mixes with water upwelling directly on the shelf. On the 16th of September 1999, water temperature close to the mouth of the Ría was colder than over the adjacent shelf and than within the Ría, suggesting that under strong upwelling conditions, deep water outcrops more intensely at this site.

The distribution of salinity shows the influence of fresh water input in the Ría (Fig. 5A). During upwelling relaxation (20th of June 1997 and the 9th of September 1999), the influence of fresh water input on the surface layer is more marked than during upwelling conditions. This can be explained by the fact that, under stratified conditions, the fresh water mixes with surface water and remains in the surface layers. This lower salinity water then extends out over the shelf. On the other hand, during an upwelling event, the effect of fresh water input on surface water salinity will be smaller, due to the higher contribution of ENAW. On the 20th of June 1997, the less saline water extends over the entire shelf up to the shelf break, as also shown above by the TS diagrams (Fig. 4B). However, even under intense upwelling condi-

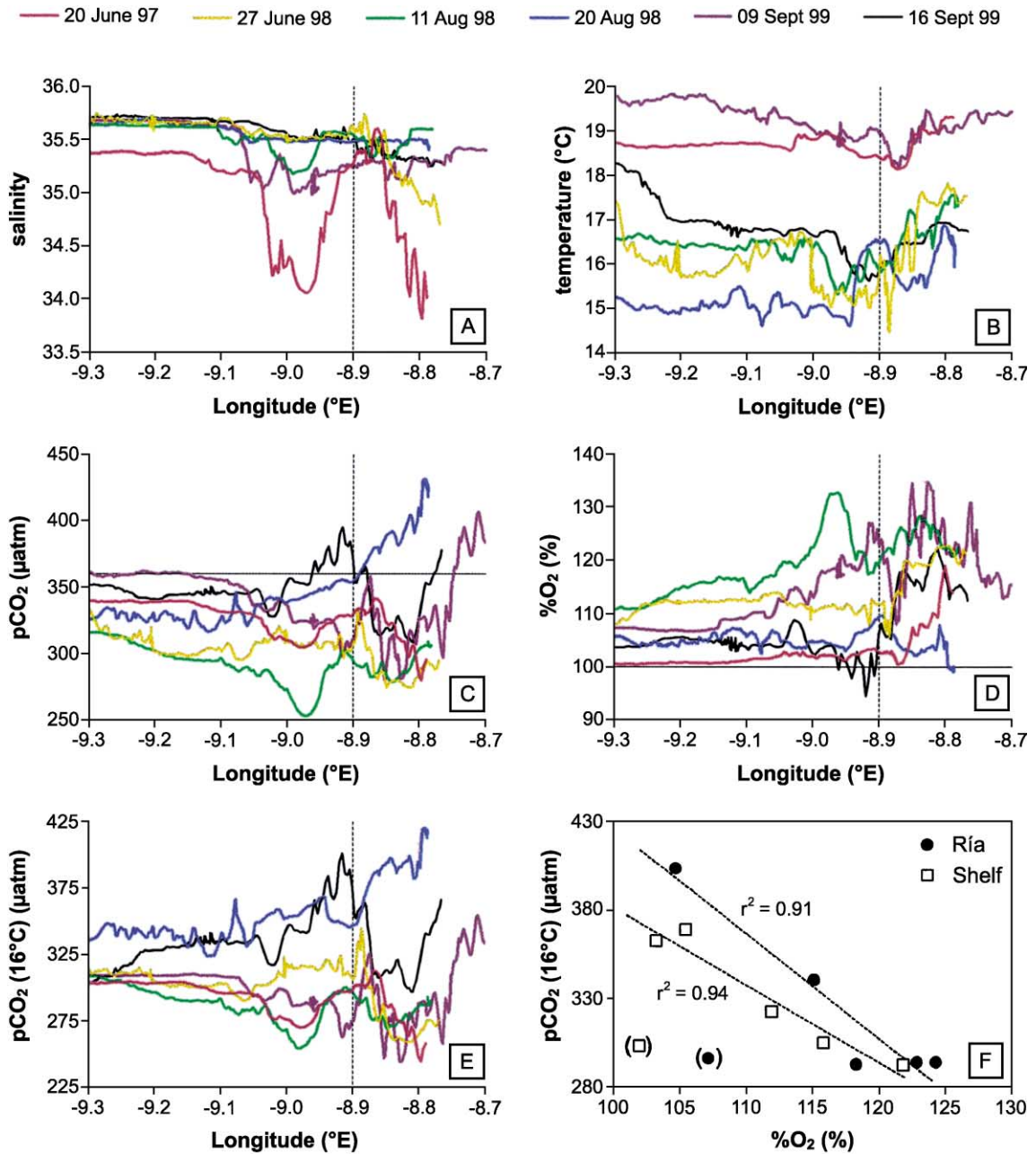


Fig. 5. Distribution of salinity, temperature ( $^{\circ}\text{C}$ ),  $p\text{CO}_2$  ( $\mu\text{atm}$ ), oxygen saturation level (%) and  $p\text{CO}_2$  normalized to  $16^{\circ}\text{C}$  ( $\mu\text{atm}$ ) along six transects from the shelf break into the Ría of Vigo, and average value (for each transect) of  $p\text{CO}_2$  normalized to  $16^{\circ}\text{C}$  versus oxygen saturation level. The points in brackets correspond to the June 1997 data and were excluded from the linear regressions (see text). The horizontal dotted line is the  $\text{CO}_2$  atmospheric equilibrium. The vertical dotted line shows the location of the mouth of the Ría of Vigo.

tions, there is a signal in the salinity distribution in the Ría and the adjacent continental shelf, as the upwelled ENAW mixes with the less saline surface water. The difference of average salinity values between the outer continental shelf (between  $-9.3^{\circ}\text{E}$  and  $-9.1^{\circ}\text{E}$ ) and the inner continental shelf (between  $-9.1^{\circ}\text{E}$  and  $-8.9^{\circ}\text{E}$ ) is  $\sim 0.12$  during active upwelling conditions (27th of June 1998, 11th of August 1998, 20th of August 1998 and 16th of September 1999) and  $\sim 0.60$  during upwelling relaxation conditions (20th of June 1997 and the 9th of September 1999), showing that the influence of outwelled water is more important on the inner continental shelf than on the outer continental shelf.

The distribution of  $p\text{CO}_2$  shows moderate seasonal variability over the outer continental shelf (range 319–360  $\mu\text{atm}$ ) and intense variability within the Ría and over the inner continental shelf (range 250–425  $\mu\text{atm}$ ) (Fig. 5C). It is also clear that the distribution of  $p\text{CO}_2$  is fairly homogeneous for a given transect over the outer continental shelf while showing strong gradients at the vicinity of the Ría. In the outer continental shelf,  $p\text{CO}_2$  values are higher on the 9th of September 1999, i.e. strong upwelling relaxation event, than on both the 20th of August 1998 and 16th of September 1999, i.e. strong upwelling events. This due to the temperature effect on equilibrium constants because the two transects carried out under strong upwelling events show higher  $p\text{CO}_2$  (16  $^{\circ}\text{C}$ ) values than the others (Fig. 5E). Both  $p\text{CO}_2$  and  $p\text{CO}_2$  (16  $^{\circ}\text{C}$ ) show higher values within the Ría than over the adjacent continental shelf on the 20th of August, illustrating the effect of upwelling within the Ría. During the two upwelling relaxation events (20th of June 1997 and the 9th of September 1999) and some of the upwelling events (27th June 1998 and 16th of September 1999),  $p\text{CO}_2$  and  $p\text{CO}_2$  (16  $^{\circ}\text{C}$ ) values are lower within the Ría of Vigo than on the adjacent continental shelf. This is related to primary production as corroborated by the distribution  $\% \text{O}_2$  that shows in general higher values within the Ría (Fig. 5D) and by the good correlation between  $p\text{CO}_2$  (16  $^{\circ}\text{C}$ ) and  $\% \text{O}_2$  (Fig. 5F). It should also be noted that for all transects,  $\% \text{O}_2$  values are almost always above the saturation level, showing that during both active upwelling and upwelling relaxation events, primary production strongly affects surface parameters and induces the observed undersaturation of  $\text{CO}_2$  over the continental shelf (Fig. 5F). The exception is the

transect of the 20th of June 1997 when  $\% \text{O}_2$  values were very close to saturation (points in brackets in Fig. 5F). This can be explained by the fact that primary production was low during this strong upwelling relaxation event and that air–sea exchange tended to bring  $\text{O}_2$  close to saturation (the effect of air–sea exchange on the  $p\text{CO}_2$  values is weaker than on the  $\text{O}_2$  values because of the carbonate buffering capacity of seawater).

We can conclude from both Sections 3.2.1 and 3.2.2 that during both downwelling conditions and upwelling conditions the undersaturation of  $\text{CO}_2$  in the continental shelf waters adjacent to the Rías is related to primary production. During downwelling conditions, the strongly  $\text{CO}_2$  undersaturated outwelled water from the Rías affect the inner adjacent continental shelf. However, the outwelling from the Rías has little effect on the outer continental shelf, except during extreme relaxation events. During upwelling conditions, oversaturation of  $\text{CO}_2$  is only observed within the Rías and  $\text{CO}_2$  undersaturation is observed in the adjacent inner and outer continental shelf. Even under strong upwelling conditions, primary production maintains  $p\text{CO}_2$  below the saturation level in the RBA.

### 3.3. Effect of shelf topography on the surface distribution of dissolved inorganic carbon

If the outwelling from the Rías only influences the distribution of  $p\text{CO}_2$  in the inner continental shelf during upwelling relaxation events, then, another process seems also to contribute to the different  $p\text{CO}_2$  and temperature-averaged values systematically observed in the RBA and CFA. Apart from the presence of the Rías, one of the differences between the CFA and the RBA is the width of the continental shelf. In the CFA, the shelf width varies between 16 and 18 km while in the RBA, the shelf is always more than 30 km wide. The ratio between the surface area and the length of the shelf break is 21 (785  $\text{km}^2/37$  km) and 37 (3365  $\text{km}^2/92$  km) for the CFA and the RBA, respectively (see Fig. 1). The flow of upwelled water is limited by the length of the shelf break, so that the volume of water upwelled on to shelf related to the water volume over the shelf will be higher in the CFA than in the RBA. This will in turn affect the distribution of surface parameters.

We computed theoretically the evolution of surface water temperature and DIC, during the onset of an upwelling event using for initial conditions the values from a cruise carried out in January 1998 (see Borges and Frankignoulle, in press, for a general description of the hydrographic conditions), i.e. mixed layer depth = 40 m,  $p\text{CO}_2 = 335 \mu\text{atm}$ , surface water temperature =  $15.6^\circ\text{C}$  and  $\text{DIC} = 2.059 \text{ mmol kg}^{-1}$ . To keep the computations as simple as possible, we considered that the salinity and TALK on the shelf and of upwelled water are the same and equal to 35.7 and  $2.340 \text{ mmol kg}^{-1}$ , respectively. We considered that water was upwelled from 200 m (Huthnance et al., 2002) characterized by  $p\text{CO}_2 = 386 \mu\text{atm}$ , temperature =  $12.0^\circ\text{C}$  and  $\text{DIC} = 2.118 \text{ mmol kg}^{-1}$  (based on numerous CTD profiles at the shelf-break). The volume of upwelled water was computed using the length of shelf break shown in Fig. 1 and an upwelling index of  $750 \text{ m}^3 \text{ km}^{-1} \text{ s}^{-1}$ , which corresponds to the flow of upwelled water per kilometer of coastline. The variation of temperature and DIC were computed by iteration during 7 days (half of the typical period of an upwelling cycle) by considering that a volume of surface shelf water is exported, equivalent to the volume of upwelled water that mixes with water on the shelf. The effect of air–sea exchange of  $\text{CO}_2$  on the DIC and  $p\text{CO}_2$  was also computed iteratively using the Wanninkhof (1992) exchange coefficient, a constant wind speed of  $10 \text{ m s}^{-1}$  and an atmospheric  $p\text{CO}_2$  value of  $364 \mu\text{atm}$ .

Fig. 6A shows that in 7 days, the decrease of surface water temperature related to upwelling is more pronounced in the CFA than in the RBA. The evolution of DIC was computed for two situations: in absence of primary production and by taking into account a net primary production rate of  $750 \text{ mg C m}^{-2} \text{ day}^{-1}$ . Fig. 6B shows, as expected, surface DIC values increasing in relation to upwelling in both areas, but the increase in the CFA is more pronounced than in the RBA even when taking primary production into account. The evolution of  $p\text{CO}_2$  was computed from the one of DIC, and in absence of primary production,  $p\text{CO}_2$  increases in both areas although more rapidly in the CFA. When taking into account primary production,  $p\text{CO}_2$  decreases in the RBA while it increases in the CFA. However, the decrease of  $p\text{CO}_2$  in the RBA is thermodynamically controlled by the decrease of temperature as shown by the increase of  $p\text{CO}_2$  ( $16^\circ\text{C}$ ) (Fig. 6D). It should be noted that the increase of DIC and  $p\text{CO}_2$

values related to the input of atmospheric  $\text{CO}_2$  from air–sea exchange is very low at this time scale. Indeed, the final values of DIC and  $p\text{CO}_2$  (from day 7) are on average (for the four simulations)  $0.8 \mu\text{mol kg}^{-1}$  and  $1.4 \mu\text{atm}$  higher, respectively, than those computed from simulations that do not take air–sea exchange into account (not shown). As expected, the most marked difference between simulations with and without taking air–sea exchange into account is for the simulation of the RBA with primary production due to the stronger air–sea  $p\text{CO}_2$  gradient but still remains negligible ( $1.1 \mu\text{mol kg}^{-1}$  and  $1.8 \mu\text{atm}$  for DIC and  $p\text{CO}_2$ , respectively).

If one takes the DIC values from day 7 of the computation made in absence of primary production, and one calculates the primary production rate needed to maintain DIC unchanged (steady state), one obtains 1570 and  $1110 \text{ mg C m}^{-2} \text{ day}^{-1}$  for the CFA and the RBA, respectively. This means that the lower DIC and  $p\text{CO}_2$  values in the RBA than in the CFA are not necessarily related to a higher primary production rate at CFA than in the RBA. Indeed, the primary production rate is expected to be higher in the CFA than RBA since the input of nitrate should be higher also in relation to width of the continental shelf.

Finally, it should be noted that at the start of the next upwelling cycle, initial  $p\text{CO}_2$  and temperature conditions will be different in the two hydrographic regions and, thus, the contrast will be emphasized.

The purpose of these simple computations is not to provide a realistic description of the evolution of parameters during the onset of an upwelling event; however, they illustrate that the observed differences between the two hydrographic areas can, to some extent, be explained by the difference of the width of the continental shelf. For instance, these computations can explain the relatively lower temperature and higher DIC and  $p\text{CO}_2$  observed values in the CFA than in the RBA. Other processes probably also contribute to enhanced upwelling in the CFA. For instance, Haynes et al. (1993) point out the increase of wind stress at Cape Finisterre, due to orographic effects, to explain the distribution of upwelling filaments off the Iberian coast. Also, off capes, upwelling can occur with a wider range of wind directions than along a relatively linear coastline (Huthnance et al., 2002). Also, it should be noted that surface seawater temperatures lower in the CFA than in the RBA is a feature that can be noticed in

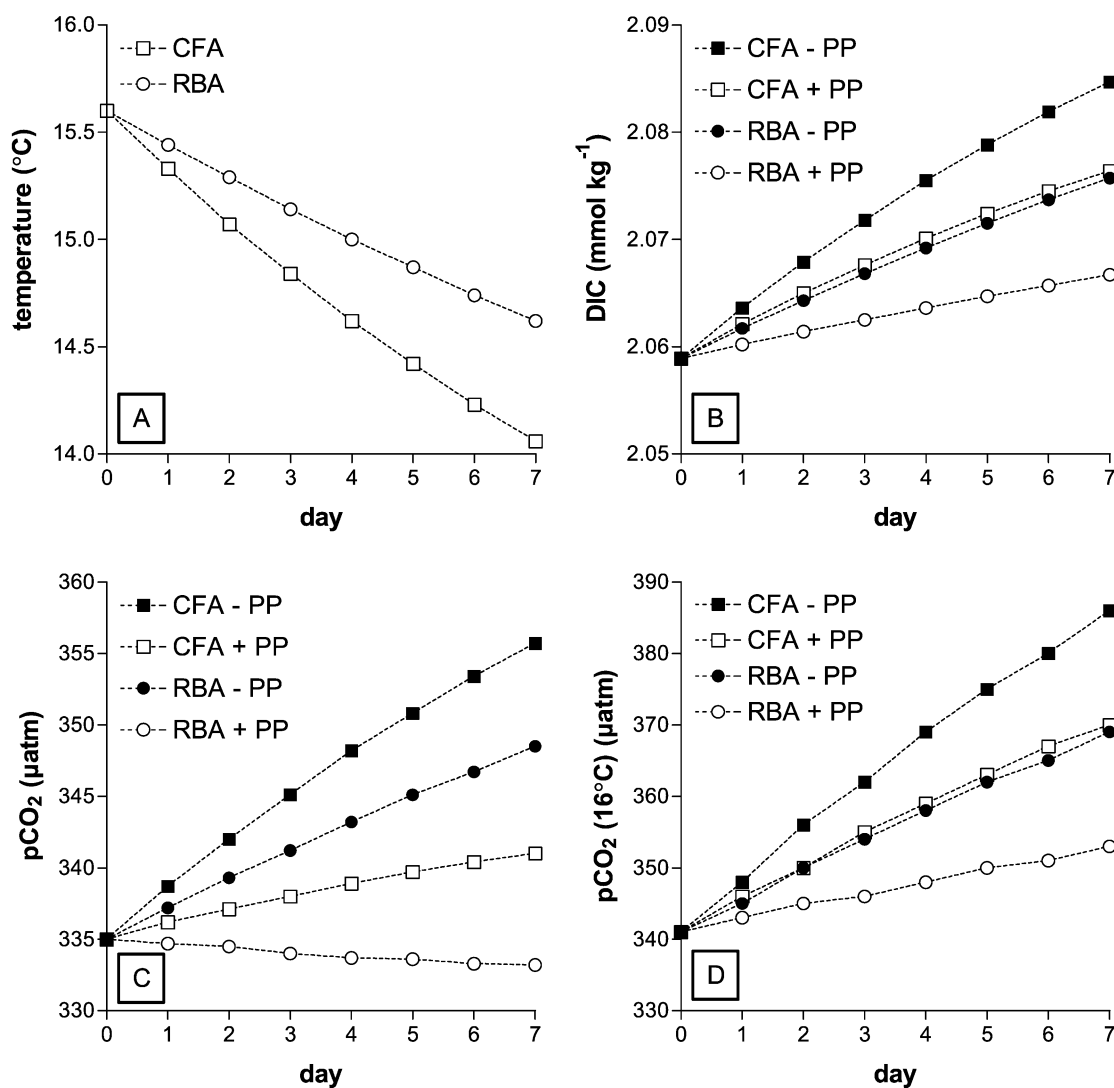


Fig. 6. Theoretical evolution of temperature (°C), DIC (mmol kg<sup>-1</sup>), pCO<sub>2</sub> (μatm) and pCO<sub>2</sub> normalized to 16 °C (μatm) in the Cape Finisterre area (CFA) and the Rías Baixas area (RBA) with the onset of an upwelling event characterised by an upwelling index of 750 m<sup>3</sup> s<sup>-1</sup> km<sup>-1</sup>, in absence of primary production (“-PP”) or taking into account a primary production rate of 750 mg C m<sup>-2</sup> day<sup>-1</sup> (“+PP”).

several published surface water temperature distributions based on field data (see Fraga, 1981; Castro et al., 1994; Tenore et al., 1995) or based on the output from “realistic” physical models (see Stevens et al., 2000).

#### 3.4. Synoptic surface distribution fields?

One of the questions that can be raised concerning the four summer cruises is whether the surface distri-

butions of parameters are synoptic or not. Borges and Frankignoulle (in press) show that temperature and pCO<sub>2</sub> can evolve rapidly within a few days in surface waters off Cape Finisterre during active upwelling conditions. This is also observed in the present work from the transects within and around the Ría of Vigo (Fig. 5). It can then be argued that the differences in surface parameters in the RBA and the CFA could be related to the fact that, for example, the former was

sampled during upwelling relaxation conditions while the latter was sampled during an active upwelling event.

For instance, during the June 1998 cruise, sampling started in the RBA in front of the Ría of Vigo and finished 9 days later in the CFA. During this

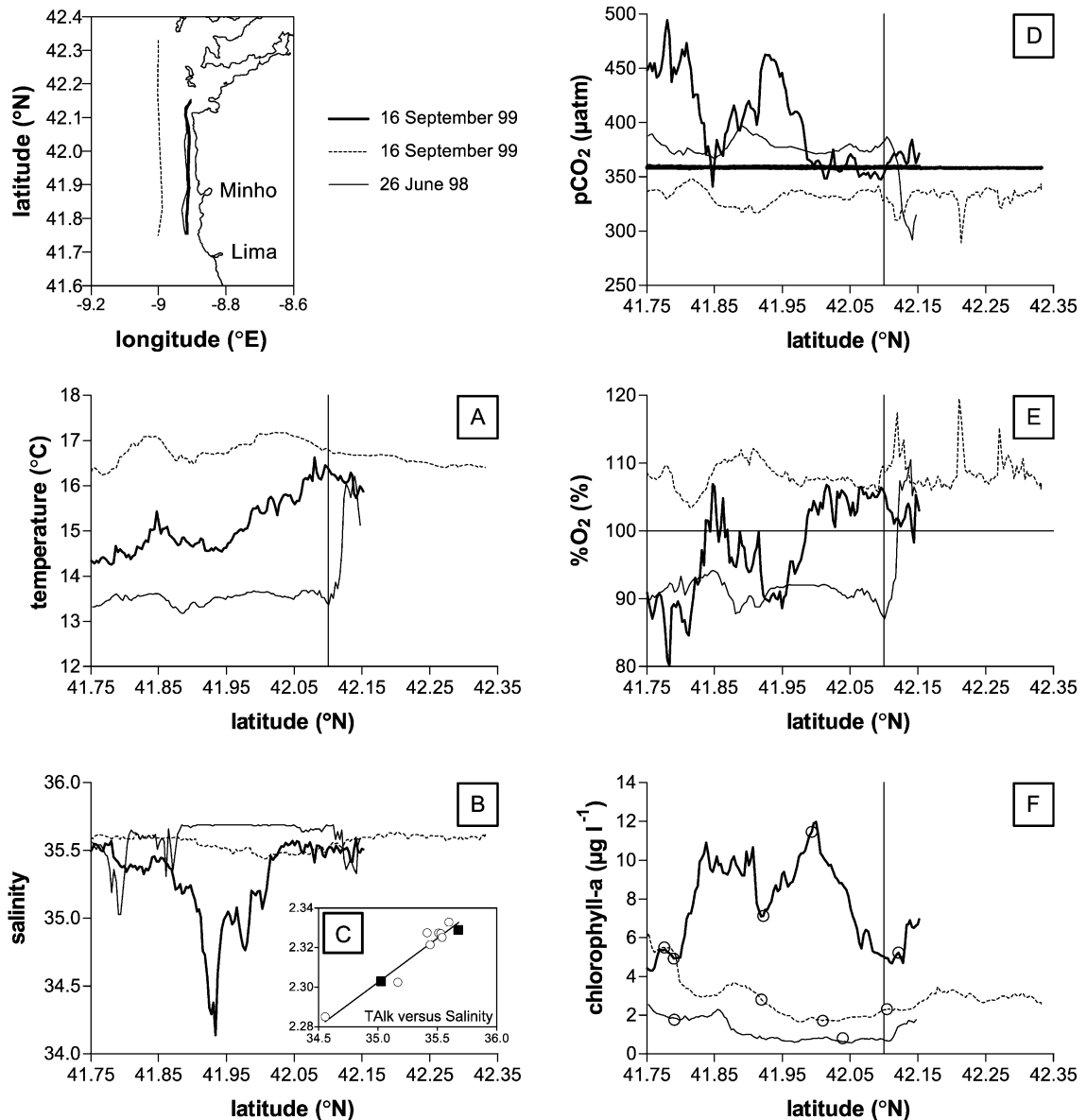


Fig. 7. Distribution of  $p\text{CO}_2$  ( $\mu\text{atm}$ ), temperature ( $^{\circ}\text{C}$ ), oxygen saturation level (%), salinity, fluorescence ( $\mu\text{g l}^{-1}$ ) and chlorophyll  $a$  concentration ( $\mu\text{g l}^{-1}$ ) versus latitude ( $^{\circ}\text{N}$ ), along three transects off the Portuguese coast. The horizontal line on the  $p\text{CO}_2$  plot corresponds to atmospheric equilibrium measured on the 16th of September 1999. In the TAlk versus salinity plot, the full squares correspond to the samples from the 26th of June 1998 and the open circles to samples from the 16th of September 1999, obtained at the same locations as the chlorophyll  $a$  samples. The solid line corresponds to the regression line:  $\text{TAlk} = 0.741 + 0.045S$  ( $r^2 = 0.937$ ,  $p < 0.0001$ ). The vertical dotted line corresponds to southernmost limit of the Rías Baixas area.

cruise, data were collected south of 42.1°N along the Portuguese coast on the day before the start of sampling in front of the Ría of Vigo (28th June 1998; Fig. 7). Temperature along the Portuguese coast is relatively constant around 13.5 °C, clearly showing the effect of upwelling (Fig. 7A). This is corroborated by the CO<sub>2</sub> oversaturation (average  $p\text{CO}_2$  of 380  $\mu\text{atm}$ ) and the %O<sub>2</sub> undersaturation (Fig. 7D,E). In the RBA (north of 42.1°N), temperature and %O<sub>2</sub> rapidly increase by about 2.5 °C and 19%, respectively, while  $p\text{CO}_2$  decreases by about 90  $\mu\text{atm}$ . These abrupt variations can be attributed to the outwelling of water from the Ría of Vigo, as shown in Fig. 7B, by the slight decrease in salinity. However, this transect clearly shows that upwelling was occurring at the start

of the June 1998 cruise and that the differences observed between the CFA and the RBA (Table 1) were not due to a data integration problem (non-synoptic field).

Fig. 7 also shows two transects along the Portuguese coast carried out during the second leg of the September 1999 cruise. Along the near-shore transect, there is a distinct signal in the salinity distribution that is related to the input of fresh water from the river Minho. Oversaturation of CO<sub>2</sub> and undersaturation of O<sub>2</sub> are associated to this water mass as described for other river plumes (e.g. Frankignoulle et al., 1998; Borges and Frankignoulle, 1999). The input of fresh water is more pronounced than during the June 1998 transect and located slightly south probably due to the

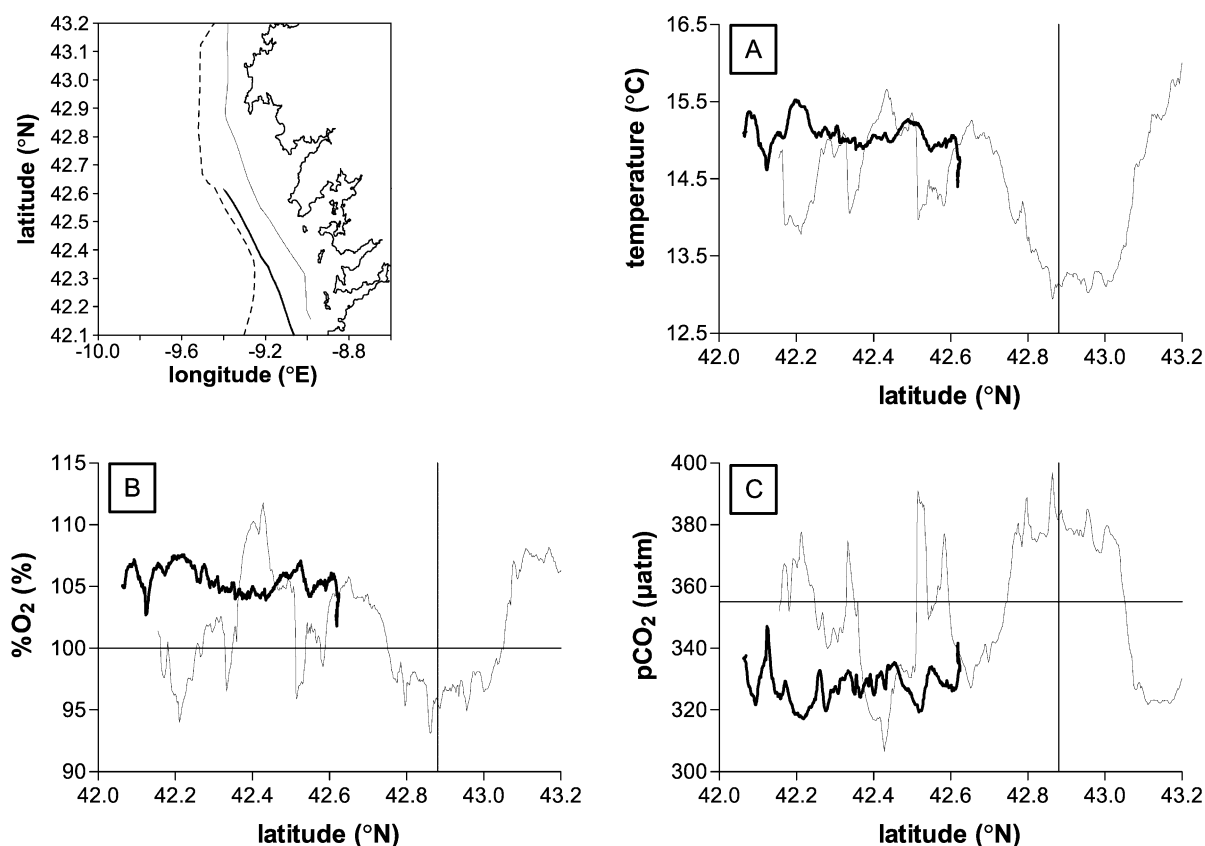


Fig. 8. Distribution of temperature (°C),  $p\text{CO}_2$  ( $\mu\text{atm}$ ) and oxygen saturation level (%) versus latitude (°N) along two transects carried out off the Galician coast on the 21st of August 1998. The horizontal dotted line corresponds to CO<sub>2</sub> atmospheric equilibrium. The vertical dotted line corresponds to the boundary between the Rías Baixas area and the Cape Finisterre area. Dotted line in map corresponds to the shelf edge (200 m isobath).

deflection of the river plume by the residual current. The plot of TALK versus salinity (Fig. 7C) shows that the river end member of the river Minho is characterised by low Total Alkalinity values. This plot also allows to check that the same river plume was sampled along the 1998 and 1999 transects and suggests that the river Lima located south of the transects was not influencing the area. However, south of 41.85°N, the salinity distribution shows that the influence of the river Minho is negligible and the strong oversaturation in CO<sub>2</sub> is associated to cold upwelled water. The signal of upwelling in temperature and *p*CO<sub>2</sub> is weaker in the RBA than along the Portuguese coast. Along the second transect on the 16th of September 1999 carried out about 9 km from the coast, surface parameters are relatively constant and temperature is higher and *p*CO<sub>2</sub> lower than near-shore. The distribution of chlorophyll *a* shows that the phytoplanktonic biomass is higher near-shore probably due to the input of nutrients by upwelling. This shows that along the Portuguese coast, active upwelling is confined to a relatively narrow near-shore tongue of water. It also shows that the second leg of the September 1999 cruise corresponded to a strong active upwelling event and that the lower *p*CO<sub>2</sub> and higher temperatures in the RBA than in the CFA (Table 1) are not related to a bias in data integration.

Fig. 8 shows two transects carried out on the 21st of August 1998 that also allow to discuss the difference between the RBA and the CFA from the point of view of synopticity since both areas were sampled within a few hours. These transects were carried out during a strong upwelling event as shown by the low temperatures measured in the CFA (see also Table 1). Overall, in the RBA, the temperature and %O<sub>2</sub> are higher and *p*CO<sub>2</sub> lower than in the CFA (Fig. 8A–C). The distribution of these parameters is very irregular in the RBA as upwelled water seems to outcrop to the surface more intensely at some locations than others. The transect carried out close to the shelf break in the RBA shows a more homogeneous distribution of parameters than near-shore, with overall slightly warmer water with lower *p*CO<sub>2</sub> values. This transect also shows that the differences between the RBA and the CFA are observed even under strong upwelling conditions and are independent of data integration.

#### 4. Conclusions

The analysis of surface water *p*CO<sub>2</sub> versus temperature from two selected cruises carried out during upwelling conditions shows that the distribution of *p*CO<sub>2</sub> over the continental shelf waters off the Galician coast is controlled by two processes that have opposite effects: the input from upwelling of deep cold water with a high CO<sub>2</sub> content and primary production. In nitrate-depleted surface waters, the distribution of *p*CO<sub>2</sub> is mainly controlled by temperature change.

The continental shelf off the Galician coast can be divided from the point of view of dissolved inorganic carbon into two distinct hydrographic regions: the Rías Baixas area and the Cape Finisterre area. The (spatially) averaged *p*CO<sub>2</sub> values are systematically lower and temperature values higher in the Rías Baixas area than in the Cape Finisterre area. The analysis of transects carried out along the Portuguese coast on two occasions and of a transect covering both hydrographic regions within a few hours indicate that this is not related to the integration of data obtained over a relatively large time span (typical cruise duration ~ 10 days).

The difference between the two hydrographic regions is mainly related to the combination of the outwelling from the Rías and the width of the continental shelf. The effect of outwelling from the Rías was investigated from vertical profile data in front of the Ría of Vigo and six transects covering the Ría and the adjacent continental shelf. Outwelling of strongly CO<sub>2</sub> undersaturated water affects significantly during upwelling relaxation events the adjacent inner continental shelf but to a much lesser extent the outer continental shelf. Furthermore, during active upwelling events, over the inner continental shelf, the outwelled water mixes with surrounding shelf water and with ENAW that upwells directly on the shelf.

In the Cape Finisterre area, the continental shelf is narrower than in the Rías Baixas area. Also, the ratio between the surface area and the length of the shelf break is lower in the Cape Finisterre area. This implies that the ratio between the volume of upwelled water to the volume of water on the shelf is higher in the Cape Finisterre area. Very simple simulations show that the lower temperature and higher *p*CO<sub>2</sub> values in the Cape Finisterre area can be explained to some extent by this topographic feature.



## Acknowledgements

The authors would like to thank the officers and crew of the *R.V. Belgica* and the *R.R.S. Charles Darwin* for the welcome on board, X.A. Álvarez-Salgado (IIM, Spain), L. Chou (ULB, Belgium) and M. Elskens (VUB, Belgium) for sharing data, MUMM (Belgium) and RVS (UK) for the thermosalinograph data, C. Daemers (ULg, Belgium) for oxygen analysis, R. Biondo and E. Libert (ULg, Belgium) for technical assistance, J. Loncar and A. Fairclough (BODC, UK) for data management and two anonymous reviewers for pertinent comments that greatly improved the quality of a previous version of the manuscript. This work was funded by the European Commission (OMEX II project, MAST programme, contract MAS3-CT97-0076). Alberto Vieira Borges received financial support from the Fonds pour la Formation à la Recherche dans l'Industrie et l'Agriculture (Belgium) and the European Commission (EUROTROPH project, No. EVK3-CT-2000-00040). Michel Frankignoulle is a research associate at the Fonds National de la Recherche Scientifique (Belgium). This is Eloise contribution number 256/27.

## References

- Alongi, D.M. (Ed.), 1988. In: Coastal Ecosystem Processes. CRC Press, New York, 419 pp.
- Álvarez-Salgado, X.A., Rosón, G., Pérez, F.F., Pazos, Y., 1993. Hydrographic variability off the Rías Baixas (NW Spain) during the upwelling season. *J. Geophys. Res.* 98 (C8), 14445–14447.
- Álvarez-Salgado, X.A., Doval, M.D., Pérez, F.F., 1999. Dissolved organic matter in shelf waters off the Ría de Vigo (NW Iberian upwelling system). *J. Mar. Syst.* 18, 383–394.
- Álvarez-Salgado, X.A., Doval, M.D., Borges, A.V., Joint, I., Frankignoulle, M., Woodward, E.M.S., Figueiras, F.G., 2002. Off-shelf fluxes of labile materials by an upwelling filament in the NW Iberian upwelling system. *Prog. Oceanogr.* 51 (2–4), 321–337.
- Arar, E.J., Collins, G.B., 1997. In vitro determination of chlorophyll *a* and pheophytin *a* in marine and freshwater phytoplankton by fluorescence. Methods for the Determination of Chemical Substances in Marine and Estuarine Environmental Matrices, vol. 445. US Environmental Protection Agency, Cincinnati, pp. 1–22.
- Bakker, D.C.E., de Baar, H.J.W., de Jong, E., 1999. The dependence on temperature and salinity of dissolved inorganic carbon in the East Atlantic surface waters. *Mar. Chem.* 65, 263–280.
- Benson, B.B., Krause, D., 1984. The concentration and isotopic fractionation of oxygen dissolved in freshwater and seawater in equilibrium with the atmosphere. *Limnol. Oceanogr.* 29, 620–632.
- Borges, A.V., Frankignoulle, M., 1999. Daily and seasonal variations of the partial pressure of CO<sub>2</sub> in surface seawater along the Belgian and southern Dutch coastal areas. *J. Mar. Syst.* 19, 251–266.
- Borges, A.V., Frankignoulle, M., 2002a. Distribution of surface carbon dioxide and air–sea exchange in the upwelling system off the Galician coast. *Global Biogeochem. Cycles*, in press.
- Borges, A.V., Frankignoulle, M., 2002b. Short-term variations of the partial pressure of CO<sub>2</sub> in surface waters of the Galician upwelling system. *Prog. Oceanogr.* 51 (2–4), 208–302.
- Castro, C.G., Pérez, F.F., Álvarez-Salgado, X.A., Rosón, G., Ríos, A.F., 1994. Hydrographic conditions associated with the relaxation of an upwelling event off the Galician coast (NW Spain). *J. Geophys. Res.* 99 (C3), 5135–5147.
- Copin-Montégut, C., 1988. A new formula for the effect of temperature on the partial pressure of carbon dioxide in seawater. *Mar. Chem.* 25, 29–37.
- Copin-Montégut, C., Raimbault, P., 1994. The Peruvian upwelling near 15°S in August 1986: results of continuous measurements of physical and chemical properties between 0 and 200 m depth. *Deep-Sea Res., Part I* 41, 439–467.
- Copin-Montégut, C., Avril, B., 1995. Continuous measurements in surface water of the Northeastern tropical Atlantic. *Tellus* 47B, 86–92.
- Culkin, F., 1965. The major constituents of seawater. In: Riley, J.P., Skirrow, G. (Eds.), *Chemical Oceanography*, vol. 2. Academic Press, London, pp. 121–161.
- Dickson, A.G., 1990. Thermodynamics of the dissociation of boric acid in synthetic sea water from 273.15 to 298.15 K. *Deep-Sea Res.* 37, 755–766.
- Dickson, A.G., 1993. pH buffers for seawater media based on the total hydrogen ion concentration scale. *Deep-Sea Res.* 40, 107–118.
- DOE, 1994. In: Dickson, A.G., Goyet, C. (Eds.), *Handbook of Methods for the Analysis of the Various Parameters of the Carbon Dioxide System in Sea Water*. US Department of Energy, Oak Ridge, ORNL/CDIAC-74.
- Doval, M.D., Álvarez-Salgado, X.A., Pérez, F.F., 1997. Dissolved organic matter in a temperate embayment affected by coastal upwelling. *Mar. Ecol. Prog. Ser.* 157, 21–37.
- Fraga, F., 1981. Upwelling off the Galician coast, Northwest Spain. In: Richards, F.A. (Ed.), *Coastal Upwelling. Coastal and Estuarine Science*, vol. 1. AGU, Washington, DC, pp. 176–182.
- Fraga, F., Mourinho, C., Manríquez, M., 1982. Las masas de agua en la costa de Galicia: junio–octubre. *Res. Exp. Cient.* 10, 51–77.
- Frankignoulle, M., Borges, A.V., 2001. European continental shelf as a significant sink for atmospheric carbon dioxide. *Global Biogeochem. Cycles* 15 (3), 569–576.
- Frankignoulle, M., Abril, G., Borges, A., Bourge, I., Canon, C., Delille, B., Libert, E., Théate, J.-M., 1998. Carbon dioxide emission from European estuaries. *Science* 282, 434–436.
- Frankignoulle, M., Borges, A., Biondo, R., 2001. A new design of equilibrator to monitor carbon dioxide in highly dynamic and turbid environments. *Water Res.* 35/5, 1344–1347.
- Gattuso, J.-P., Frankignoulle, M., Wollast, R., 1998. Carbon and carbonate metabolism in coastal aquatic ecosystems. *Annu. Rev. Ecol. Syst.* 29, 405–433.

- Goyet, C., Millero, F.J., O'Sullivan, D.W., Eischeid, G., McCue, S.J., Bellerby, R.G.J., 1998. Temporal variations of  $p\text{CO}_2$  in surface seawater of the Arabian Sea in 1995. *Deep-Sea Res.* 45, 609–623.
- Haynes, R., Barton, E.D., Pilling, I., 1993. Development, persistence, and variability of upwelling filaments off the Atlantic coast of the Iberian Peninsula. *J. Geophys. Res.* 98 (C12), 22681–22692.
- Huthnance, J.M., van Aken, H.M., White, M., Barton, E.D., Le Cann, B.L., Coelho, E.M., Fanjul, E.A., Miller, P., Vitorino, J., 2002. Ocean margin exchanges—water flux estimates. *J. Mar. Syst.* 32 (this issue).
- Keeling, C.D., Whorf, T.P., 1999. Atmospheric  $\text{CO}_2$  records from sites in the SIO air sampling network. *Trends: A Compendium of Data on Global Change*. Carbon Dioxide Information Analysis Center, Oak Ridge National Laboratory, US Department of Energy, Oak Ridge, TN.
- Kelley, J.J., Hood, D.W., 1971. Carbon dioxide in the Pacific Ocean and Bearing Sea: upwelling and mixing. *J. Geophys. Res.* 76, 745–753.
- Körtzinger, A., Duinker, J.C., Mintrop, L., 1997. Strong  $\text{CO}_2$  emissions from the Arabian Sea during South-West Monsoon. *Geophys. Res. Lett.* 24, 1763–1766.
- Lefèvre, N., Moore, G., Aiken, J., Watson, A., Cooper, D., Ling, R., 1998. Variability of  $p\text{CO}_2$  in the tropical Atlantic in 1995. *J. Geophys. Res.* 103 (C3), 5623–5634.
- Liss, P.S., Merlivat, L., 1986. Air–sea exchanges rates: introduction and synthesis. In: *Buat-Ménard, P. (Ed.), The Role of Air–Sea Exchange in Geochemical Cycling*. NATO ASI Series, Reidel, Utrecht, pp. 113–128.
- Nogueira, E., Pérez, F.F., Ríos, A.F., 1997. Modelling thermohaline properties in an estuarine upwelling ecosystem (Ría of Vigo: NW Spain) using Box–Jenkins transfer function models. *Estuarine, Coastal Shelf Sci.* 44, 685–702.
- Nogueira, E., Pérez, F.F., Ríos, A.F., 1998. Modelling nutrients and chlorophyll *a* time series in an estuarine upwelling ecosystem (Ría of Vigo: NW Spain) using the Box–Jenkins approach. *Estuarine, Coastal Shelf Sci.* 46, 267–286.
- Pérez, F.F., Ríos, A.F., Rosón, G., 1999. Sea surface carbon dioxide off the Iberian Peninsula (North Eastern Atlantic Ocean). *J. Mar. Syst.* 19, 27–46.
- Roy, R.N., Roy, L.N., Vogel, K.M., Porter-Moore, C., Pearson, T., Good, C.E., Millero, F.J., Cambell, D.J., 1993. Determination of the ionization constants of carbonic acid in seawater in salinities 5 to 45 and temperatures 0 to 45 °C. *Mar. Chem.* 44, 249–267.
- Sarmiento, J.L., Murnane, R., Le Quéré, C., 1995. Air–sea  $\text{CO}_2$  transfer and the carbon budget of the North Atlantic. *Philos. Trans. R. Soc. London, Ser. B* 348, 211–219.
- Simpson, J.J., 1984. On the exchange of oxygen and carbon dioxide between ocean and atmosphere in an eastern boundary current. In: *Brutsaert, W., Jirka, G.H. (Eds.), Gas Transfer at Water Surfaces*. Reidel, Dordrecht, pp. 505–514.
- Simpson, J.J., Zirino, A., 1980. Biological control of pH in the Peruvian coastal upwelling area. *Deep-Sea Res.* 27, 234–248.
- Stevens, I., Hamann, M., Johnson, J.A., Fiúza, A.F.G., 2000. Comparison between a fine resolution model and observations in the Iberian shelf-slope region. *J. Mar. Syst.* 26, 53–74.
- Takahashi, T., Takahashi, T.T., Sutherland, S.C., 1995. An assessment of the role of the North Atlantic as a  $\text{CO}_2$  sink. *Philos. Trans. R. Soc. London, Ser. B* 348, 143–152.
- Tans, P.P., Fung, I.Y., Takahashi, T., 1990. Observational constraints on the global atmospheric  $\text{CO}_2$  budget. *Science* 247, 1431–1438.
- Tenore, K.R., Alonso-Noval, M., Alvarez-Ossorio, M., Atkinson, L.P., Cabanas, J.M., Cal, R.M., Campos, H.J., Castillejo, F., Chesney, E.J., Gonzalez, N., Hanson, R.B., McClain, C.R., Miranda, A., Roman, M.R., Sanchez, J., Santiago, G., Valdes, L., Varela, M., Yoder, J., 1995. Fisheries and oceanography off Galicia, NW Spain: mesoscale spatial and temporal changes in physical processes and resultant patterns of biological productivity. *J. Geophys. Res.* 100 (C6), 10943–10966.
- Thomas, H., Schneider, B., 1999. The seasonal cycle of carbon dioxide in Baltic Sea surface waters. *J. Mar. Syst.* 22, 53–67.
- Tilstone, G.H., Figueiras, F.G., Fermín, E.G., Arbones, D., 1999. Significance of nanoplankton photosynthesis and primary production in a coastal upwelling system (Ría of Vigo, NW Spain). *Mar. Ecol. Prog. Ser.* 183, 13–27.
- Torres, R., Turner, D.R., Silva, N., Rutllant, J., 1999. High short-term variability of  $\text{CO}_2$  fluxes during an upwelling event off the Chilean coast at 30°S. *Deep-Sea Res., Part I* 46, 1161–1179.
- Tsunogai, S., Watanabe, S., Sato, T., 1999. Is there a “continental shelf pump” for the absorption of atmospheric  $\text{CO}_2$ ? *Tellus* 51B, 701–712.
- van Green, A., Takesue, R.K., Goddard, J., Takahashi, T., Barth, J.A., Smith, R.L., 2000. Carbon and nutrient dynamics during coastal upwelling off Cape Blanco, Oregon. *Deep-Sea Res., Part II* 47, 975–1002.
- Walsh, J.J. (Ed.), 1988. *On the Nature of Continental Shelves*. Academic Press, New York, 520 pp.
- Walsh, J.J., 1991. Importance of continental margins in the marine biogeochemical cycling of carbon and nitrogen. *Nature* 350, 53–55.
- Wang, S.-L., Chen, C.-T.A., Hong, G.-H., Chung, C.-S., 2000. Carbon dioxide and related parameters in the East China Sea. *Cont. Shelf Res.* 20, 525–544.
- Wanninkhof, R., 1992. Relationship between wind speed and gas exchange over the ocean. *J. Geophys. Res.* 97 (C5), 7373–7382.
- Weiss, R.F., 1974. Carbon dioxide in water and seawater: the solubility of a non-ideal gas. *Mar. Chem.* 2, 203–215.
- Wollast, R., 1998. Evaluation and comparison of the global carbon cycle in the coastal zone and in the open ocean. In: *Brink, K.H., Robinson, A.R. (Eds.), The Sea, vol. 10*. Wiley, New York, pp. 213–252.